IOSR Journal Of Applied Physics (IOSR-JAP)
e-ISSN: 2278-4861.Volume 13, Issue 2 Ser. II (Mar. – Apr. 2021), PP 60-69
www.Iosrjournals.Org

Effect of nano-clay on di-electric and thermal properties of polyurethane/clay nanocomposites

Dalia E. Abulyazied[a,b,*] , Basma M. Hendi[a], Hameda T. Al-Atawi[a], Ryma A. Al-Ahmari[a], Wejdan. S. Ghamdi[a]

[a] *Department of Physics, Faculty of Science, University of Tabuk, Tabuk, Saudi Arabia*
[b] *Polymer Laboratory, Petrochemical Dept., Egyptian Petroleum Research Institute, Nasr City, Cairo, Egypt.*
Corresponding author: D.E. Abulyazied

Abstract
The main object of this paper is to study the dielectric and thermal behavior of polyurethane/organoclay nanocomposites. Modification of Egyptian Bentonite (EB) was carried out using an organo-modifier namely; octadecyl amine (ODA). Polyurethane nanocomposites were synthesized with organically modified EB (Organo Bentonites OB) by in situ polymerization and compositions were prepared by a casting process. The morphology of the OB dispersion in polyurethane nanocomposites was investigated by transmission electron microscopy TEM. A thermogravimetric analyzer (TGA) was used to investigate the decomposition behavior and thermal stability of the cured nanocomposites. The thermal stability of the PNC films was significantly increased with the OB content increment. The complex dielectric permittivity, electrical conductivity, electric modulus, and impedance spectra of the PU/OB nanocomposites were investigated in the frequency range from 0.1 Hz to 10 MHz. The real and imaginary parts of the permittivity decrease with increasing frequency due to an increase in OB content. All the nanocomposites showed relatively low conductivity values and high impedance that could be used for nano-dielectrics.

Keywords*: Bentonite, Dielectric properties, Nanocomposites, Organo-clay, Polyurethane, TEM, TGA*

Date of Submission: 18-03-2021 Date of Acceptance: 01-04-2021

I. Introduction

In the last two decades, polymer nanocomposites have been gained large research attention due to their thermal, electrical[1], optical[2], and mechanical properties[3]. Especially, studying dielectric and thermal properties of polymer nanocomposite PNCs has become a fast-growing field of research because of its amazing and affluent diversity of applications like in integrated circuits, nanodielectrics, and insulating devices.[4] Polyurethane (PU) is one of the most important polymers which is an exclusive polymer with a wide range of physical and chemical properties. With well-designed combinations of monomeric materials, PUs can be tailored to meet the diversified demands of various applications such as coatings, adhesives, fibers, thermoplastic elastomers, and foams[5]. However, PUs also has some disadvantages, such as low thermal stability and low mechanical strength, etc[6]. It is well known that composites can be produced exhibiting enhanced properties that the constituent materials may not exhibit [7–10]. Nowadays, clay minerals or layered-silicates are extensively used as reinforcing materials for improving many properties of polymers such as mechanical, gas barrier, heat resistance, flame retardancy, biodegradability, and many others[11–13]. The main benefits of clay minerals as reinforcing materials are their low density, abundant availability, low cost, high aspect ratio, and large specific surface area, which causes high improvement in the properties of these polymers[5,14]. Enhanced performance is a result of the exfoliation of nano-size silicate flakes from larger aggregate particles that greatly increase the surface area of interaction between clay and polymer [15]. The strong industrial benefit of polymer/ clay nanocomposites in various applications especially, those with low dielectric constants, low dielectric losses and high thermal stability[16–18] has stimulated many researchers to keep investigations into their structure-property correlation [19–22]. In this study, we synthesized polyurethane clay nanocomposites with organically modified EB (Organo Bentonites OB). The effect of the dispersibility of organoclay on the properties of polyurethane/clay nanocomposites such as morphology, thermal stability has been studied. Moreover, the dielectric properties of the PU/OB nanocomposites were investigated at different frequencies and various weight percent of the OB.

II. Experimental

2.1. Materials

Egyptian Bentonite EB is supplied from south of El-Hamamm district, grinding through ball- mill and saving at 0.6 micron. It was dried at 80 °C for 24 h under vacuum conditions. (Reported basal plane spacing, d001 = 1:26 nm).

Octadecyl amine (ODA) CH_3 $(CH_2)_{17}NH_2$ (Mw 269.51 gm/mole), hydrochloric acid, and sodium chloride were provided by Aldrich, USA. Tolylene-2,4-diisocyanate (TDI) (Fluka, Germany). Polyethylene glycol (PEG) Mn = 600 g/mol (Fluka, Germany), OH functionality = 2.0. Methyl Ethyl Ketone (MEK)(Butanone), ADWIC Co.

2.2. Preparation of Organo–Bentonite OB :

EB was purified to remove impurities, i.e. carbonates, iron hydroxide, and organic matter, then activated to Na-B according to the method mentioned in a previous work [23]. The organo-bentonite was synthesized by ion exchange reaction between Na-bentonite and octadecyl amine (ODA). The used solution of the ammonium salt was heated at 80 °C for a few minutes. The ODA was protonated by adding HCl. Aqueous suspension 0.5 wt% of Na-B was prepared and heated also at 80 ^oC. The prepared alkylammonium salt solution was dropwise added to the Na-bentonite suspension and maintained at 80 °C for 12 h under vigorous stirring. After that, the suspension was cooled to room temperature. Finally, the processed bentonite was collected by centrifugation and then washed with deionized water many times to remove residual chlorine or cations until no halide was revealed in the filtrate by $AgNO_3$ test. The dispersion and washing was accomplished using a 50/50 ethanol/water mixture. The filter cake was then placed in a vacuum oven at 80^0C for 24 h. The dried cake was ground and screened with a 325-mesh sieve to obtain the organ bentonite OB[23].

2.3. Preparations of PU/OB nanocomposites[24]

PU/OB nanocomposites were prepared as follows: different amounts (1, 3, and 5 wt %) of OB were swelled with PEG in MEK and stirred for 1 h at 70^0C, followed by sonication for 15 min. The PEG/OB mixture was blended for a particular PU/OB nanocomposite with the calculated amount of TDI. The mixture was stirred vigorously for 1 hour at 70 ◦C. Then the PU/OB nanocomposites were obtained when the viscous products were poured into molds and left for 2 days to ensure complete removal of MEK (scheme 1).

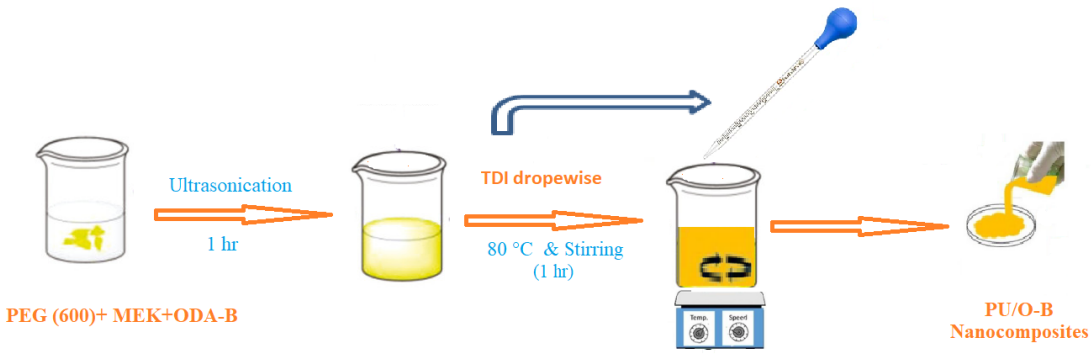

Scheme (1): PU/OB nanocomposites preparation by the in-situ intercalation polymerization mechanism

2.4. Characterizations:

Transmission electron microscopy (TEM) was adopted to characterize the nano-particles modification. TEM was performed by TEM-1230 with an accelerating voltage of 100 KV (JEOL Co., Japan). A thermogravimetric analyzer (TGA) was used to investigate decomposition behavior and thermal stability of the cured nanocomposites using a detector type: Shimadzu TGA-50H. A typical sample weight was about 8-10 mg and the analysis was performed at a heating rate of 10^oC/min from 25 to 1000 ^oC for organo-bentonite samples and from 25 to 600 for PU/OB nanocomposite samples under nitrogen atmosphere. The dielectric properties were carried out using Novocontrol high-resolution alpha analyzer.

III. Results And Discussion

3.1. Transmission Electron Microscope TEM

The TEM images of neat unmodified bentonite is presented in Figure 1-a. It is seen from this figure that the particles of unmodified bentonite are in the agglomerated forms. The TEM photograph of the prepared OB nanoparticles is shown in Figure 1-b. The figure represents nanoclay has a high spherical structure and rough surface. The average size of spherical OB nanoparticles is about 10 nm.

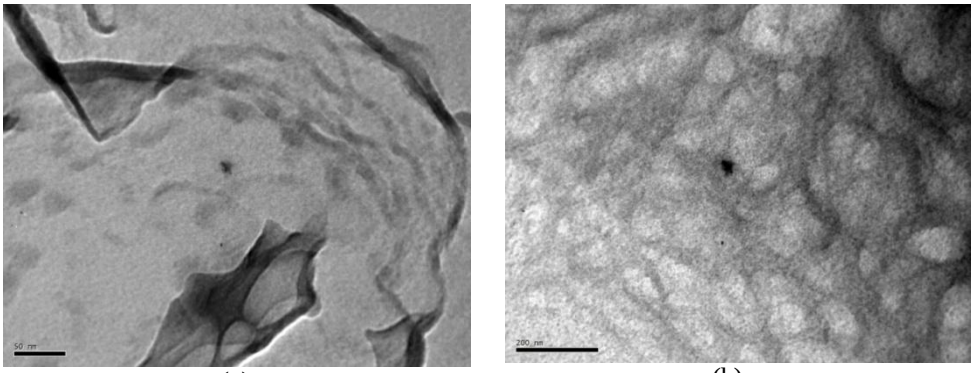

(a) (b)

Fig. 1. : TEM photographs of the EB: (a) unmodified Na-B and (b) OB

TEM images of PU/OB nanocomposites at two various OB% are illustrated in Figure 2. The micrographs, reveals that most of the organo- bentonite OB is well dispersed in the PU matrix as a separated clay particle while some OB agglomerated as tactoids Figure 2-a. It can be also observed that more aggregates are found when the OB content is increased to 5% wt, as shown in Figure 2-b. This is credible, considering that at high OB concentration, the interparticle distance is small, and hence, agglomeration of these nanoparticles can occur during mixing. Due to appropriate processing conditions and modification of bentonite used in this study, a relatively good dispersion was achieved.

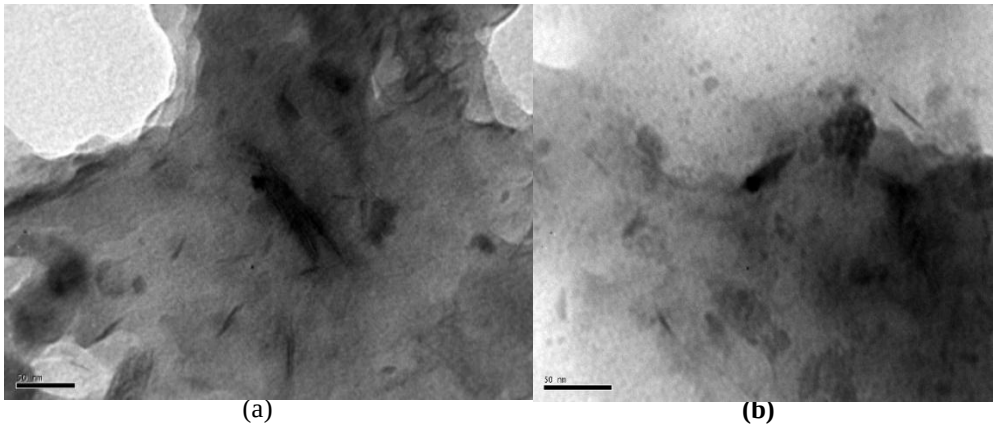

(a) **(b)**

Fig. 2. : TEM images of PU/O-B nanocomposites: (a) 1wt % (b) 5 wt% at 300 Kx.

3.2.TGA Of Nanocomposites:

The TGA thermogram of the Na-B and OB was previously discussed in detail [23]. The TGA thermograms of the pure PU and PU/OB nanocomposites are shown in Figure (3). It is clear from the figure that with the addition of the OB, the thermal stability of the PU film was significantly increased. From figure (3) the values of the temperatures at which 5% weight-loss ($T_{5\%}$) was calculated, besides the char yield at 500 ◦C for nanocomposite series was determined and shown in Table (1). Besides, The table displays the temperatures at which the maximum weight-loss occurred (T_{max}), which have been derived from the derivative thermogravimetric (DTG) Figure (4). The data shows that $T_{5\%}$ and T_{max} increases with increasing the OB content in the PU matrix. Besides, $T_{5\%}$ of PU/OB nanocomposite sample at 5wt% of OB are 20 ◦C higher than that of the pure PU. Also, T_{max} for the same PU/OB nanocomposites sample (5wt% OB) rises 18 ◦C higher than that for the pure PU. Moreover, the char yield at 500 ◦C for nanocomposite series has been boosted with the increasing of the OB content as expected. These results confirm that the thermal stability of the PU/OB nanocomposites was enhanced due to the presence of the organ bentonite. The increase in thermal stability could be attributed to the high thermal stability of bentonite and the interaction between the bentonite particles and the polyurethane matrix[25]. Moreover, the higher thermal stability of the nanocomposites has also been attributed to restricted thermal motions of the polymer localized in the galleries which reduce the rate of propagation[26–28].

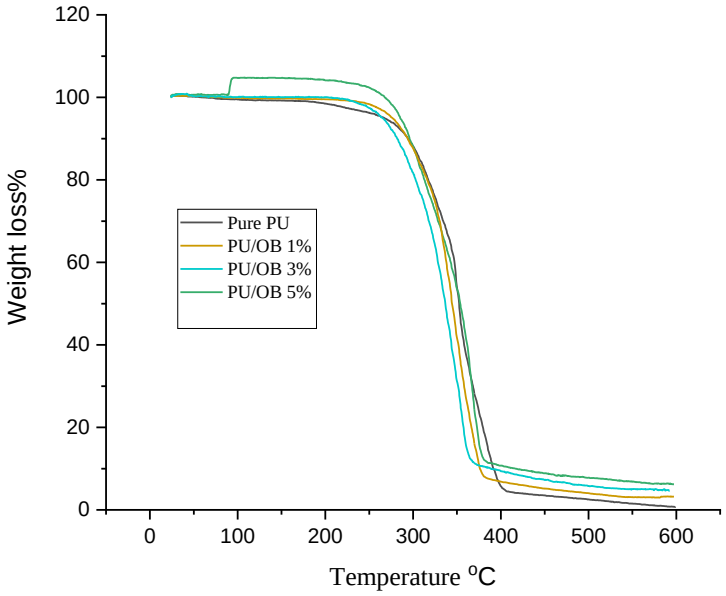

Fig.3. Thermogravimetric (TG) curves pure PU and PU/OB nanocomposites

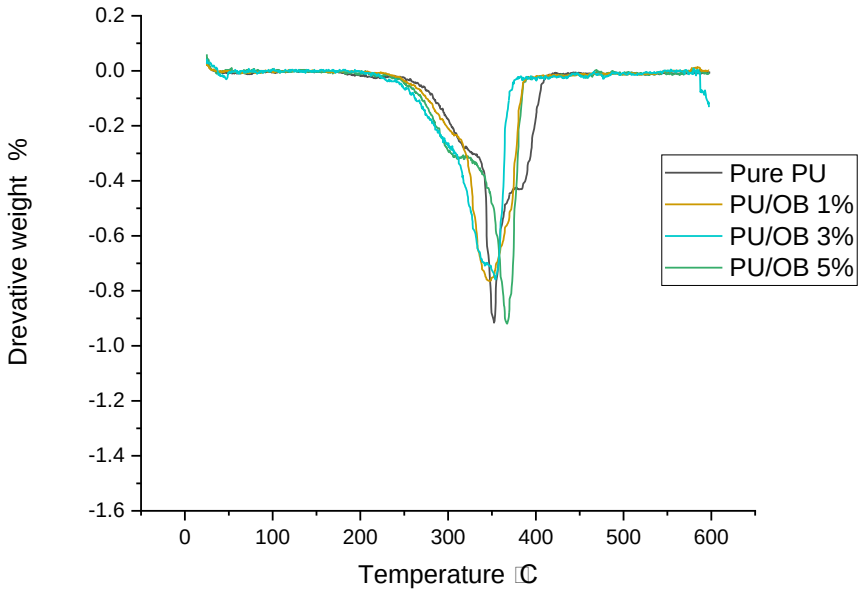

Figure 4: Derivative thermogravimetric (DTG) of Pure PU and PU/OB nanocomposites.

Table 1: Thermal parameters of pure PU and PU/OB nanocomposites.

OB%	$T_{5\,\%}$ °C	T_{max} °C	char residue (wt% at 500 °C)
0	267	352	2.4
1.00%	279	353	4.104
3.00%	280	363	6.047
5.00%	287	370	7.811

3.3. Dielectric properties of B-ODA/PU nanocomposite

Dielectric materials can be used to store electrical energy in the form of charge separation when the electron distributions around constituent atoms or molecules are polarized by an external electric field. The complex permittivity of a material can be expressed as[29,30]:

$$\varepsilon^*(\omega) = \varepsilon'(\omega) + \varepsilon''(\omega) \quad \ldots\ldots\ldots\ldots\ldots\ldots\ldots\ldots(1)$$

where(ε') and (ε'') are the real and imaginary parts of the complex permittivity and j = $\sqrt{-1}$. The magnitudes of (ε') and (ε'') depend on the frequency ω of the applied electric field. The dielectric constant (ε') as a function of the frequency for pure PU and PU/OB nanocomposites of different weight% of the OB in the frequency range, 0.1 Hz to 1 MHz at room temperature (30 °C), is presented in figure (5). It is observed from the figure that the ε′ is rapidly reduced with increasing frequency at lower frequencies region, whereas it slowly diminishes with growing frequency until it becomes frequency independent at higher frequency region. In the low-frequency region, the polymeric dipoles tend to orient themselves along the direction of the applied electric field. However, at higher frequencies, a reduction in the values of ε′, is attributed to the fact that a finite time is required by charge carriers to align themselves parallel to the applied field. Thus, at higher applied frequency, the electrons turn around more quickly, and consequently, the possibility of electrons reaching boundaries reduces severely. This causes a decrease in the polarization thereby decreasing the values of ε′ [30–32]. Otherwise, the figure manifests enhancing in ε` values by increasing OB content which may be due to fact that the bentonite surface contains hydroxyl groups, which makes it's surface polar. Moreover, this could be ascribed to the fact that nanoclay has a large surface area which in turn increases the interfacial area between polyurethane and nano -organo bentonite particles[5].

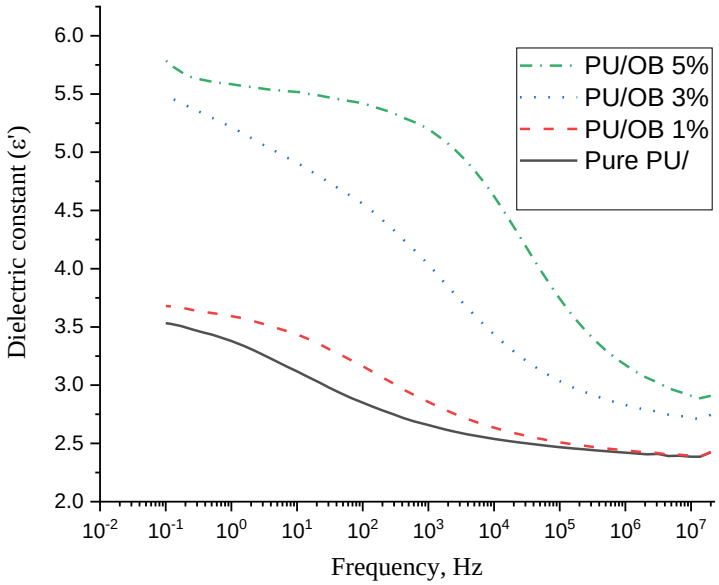

Fig.5. Frequency dependence dielectric constant of pure PU and PU\OB nanocomposites

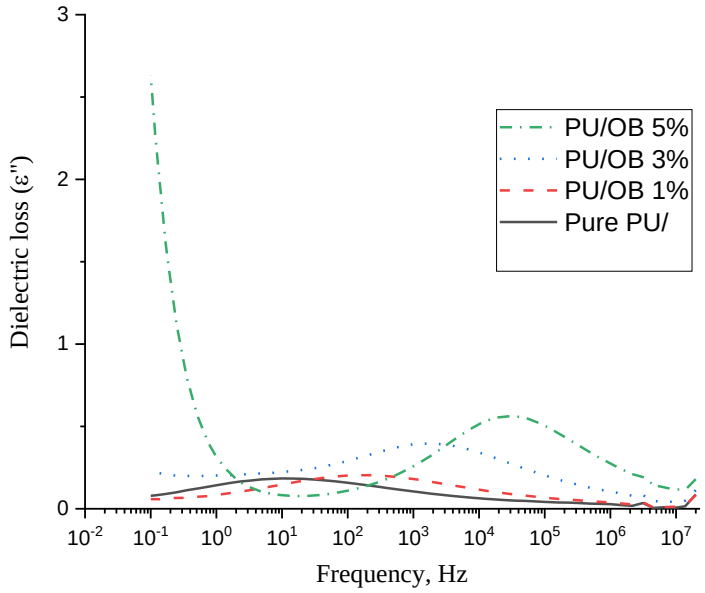

Fig.6. Frequency dependence dielectric loss of pure PU and PU\B-ODA nanocomposites

Figure (6) exhibits the variation of dielectric loss with frequency for PU/OB nanocomposites containing different amounts of OB. The loss spectra consist of peaks at a characteristic frequency which indicates the presence of relaxing dipoles in these nanocomposites[33]. It is also observed that the peak frequency is shifting towards the higher frequency side with an increase in OB wt%. As the peak shifts towards the higher frequency side, the relaxation time is decreased. By addition of bentonite, it is believed, that there is a decrease in the amorphous content of the sample. In polar polymer, it was reported that the increase in crystallinity reduces the tan δ values (and consequently reduce $\varepsilon^{"}$ so α and β relaxation process shifted to lower frequency) because the relaxation time τ is given by [34]

$$\tau_{\varepsilon} = \frac{1}{2\pi f_p} \qquad \text{.....(2)}$$

where f_p is the frequency corresponding to the maximum in relaxation peak. In PU/ OB nanocomposites, as the concentration of OB increases up to 5 wt% in these materials, the crystallinity in PU/OB nanocomposites decreases. Hence, the observed shift in relaxation frequency or reduction in relaxation time is due to the reduction in crystallinity. The calculated values of τ_{ε} values for these PU/OB materials are given in Table (2).

The complex dielectric modulus (M*) is useful to analyze the different relaxation phenomena in the polymeric system and separates the polarization effect from the bulk relaxation and relaxation due to the large contribution of electrode polarization effect. M* formalism can be determined by the following equations given below.

$$M^*(\omega) = \frac{1}{\varepsilon^*(\omega)} \qquad \text{.....(3)}$$

$$M^* = \grave{M} + jM^{"} = \frac{\grave{\varepsilon}}{\grave{\varepsilon}^2+\varepsilon^{"2}} + j\frac{\varepsilon^{"}}{\grave{\varepsilon}^2+\varepsilon^{"2}} \qquad \text{.....(4)}$$

Figure (7) and (8) depict the dependence of real and imaginary part of modulus for pure PU and PU\B-ODA nanocomposites at different wt% of OB. Figure (7) shows that the dispersion of M` occurred at a higher frequency while it tends to zero at a lower frequency indicating vanishing of electrode polarization effect at the electrode-film sample interface [35–37]. Figure (8) displays the presence of a peak at a higher frequency which is analogous to loss tangent peak, this peak is shifting to higher frequency values with an increase in OB content which can be explained as the movement of ions for a longer distance in the composites. From the frequency corresponding to the peak maximum of $M^{"}$spectra, the ion conduction relaxation time values are calculated using the relation ($\tau_M = \frac{1}{2\pi f_M}$)[38] where f_M is the ac conductivity relaxation frequency, which separates the change in ions from dc to ac transport. The calculated $\tau_M$values are represented in Table 2.

Table2: Values of relaxation times (τ_ε and τ_M) at 30 °C of pure PU and PU/OB nanocomposites

OB%	τ_ε, µs	τ_M, µs
0	4683	5136
1.00%	1137	290
3.00%	86	20
5.00%	4.5	1.6

The value of the modulus relaxation time diminishes with the increasing the OB content up to 5 wt% which is due to the increased amount of free charge carriers[39]. Further, the presence of OB may lead to increasing the free volume in the nanocomposites which improves polymer chain segmental motion. So OB has an optimum influence on the structural dynamical process in the polymer[40].

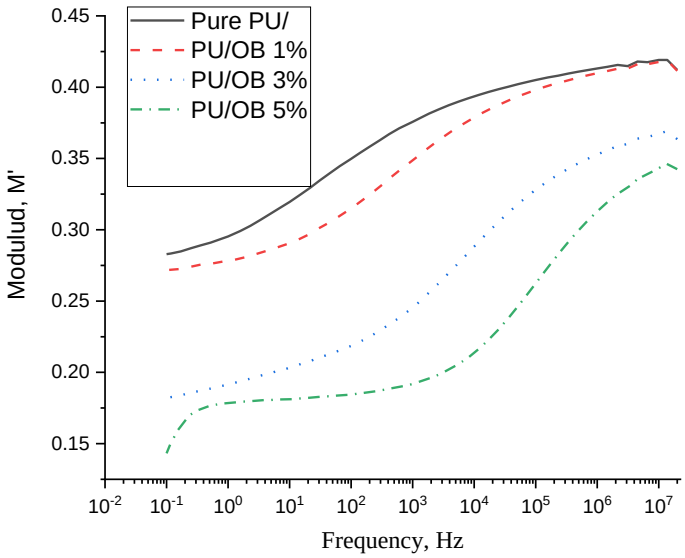

Fig.7. Frequency dependence real part of complex dielectric modulus of pure PU and PU\OB nanocomposites

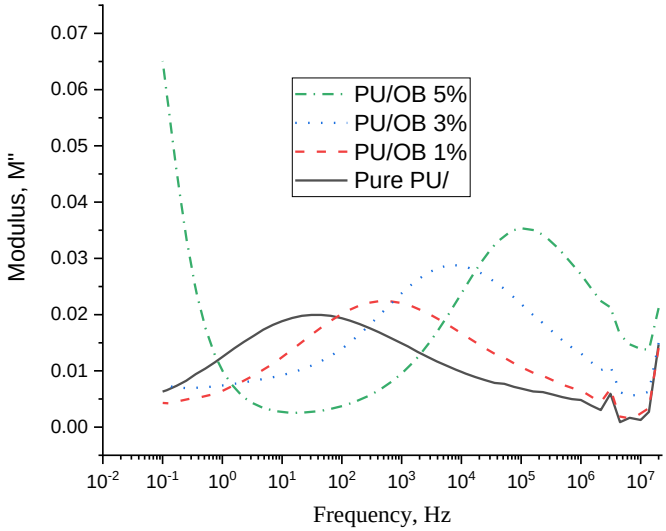

Fig.8. Frequency dependence imaginary part of complex dielectric modulus of pure PU and PU\OB nanocomposites

The real σ′ and imaginary σ″ parts of complex ac electrical conductivity σ*(ω), as well as the resistive Z′ and capacitive reactance Z″ parts of complex impedance Z*(ω) as a function of frequency for the pure PU and PU/OB nanocomposites at room temperature, are shown in Fig. (9 and 10) respectively. Figure 9, clarify that the complex conductivity of all pure and PU/OB nanocomposites varies linearly with the frequency boost. The increase of conductivity with frequency rise is due to the polarization effects resulted from the accumulation of charge at the electrode by the slow reversal of the applied electric field. Otherwise, figure 10, shows that all samples possess relatively low conductivity values (~ 10^{-14} to 10^{-6} S/cm) over the frequency range from 0.1 Hz to 1 MHz [40]. Figure 10, illustrates the megaohm impedance values of the samples at audio frequencies for these PNCs promote their good electrical insulation properties, Moreover, the Z″> Z′ confirms the prevailing capacitive manner of these nanocomposites which can be used for energy storage applications[41].

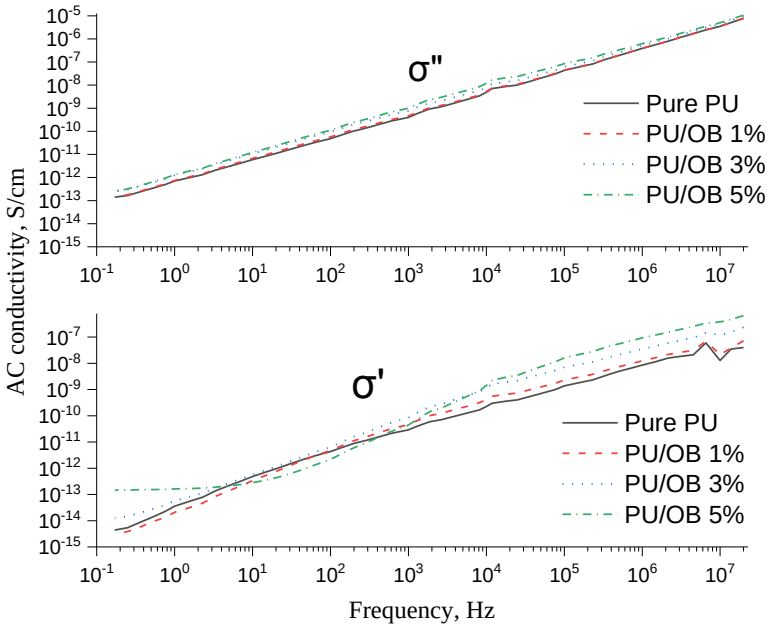

Fig.9. Frequency dependence real and imaginary parts of complex of Ac conductivity of pure PU and PU\OB nanocomposites

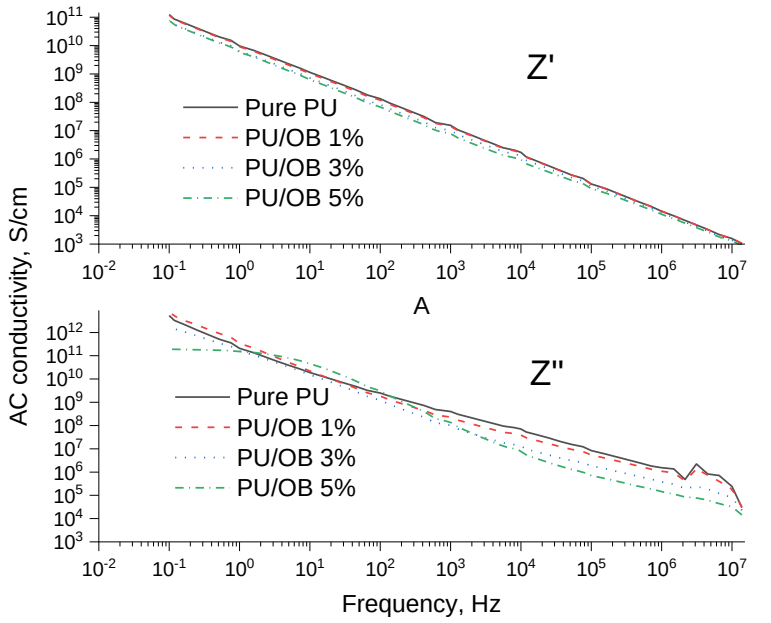

Fig.10. Frequency dependence real and imaginary parts of complex impedance of pure PU and PU\OB nanocomposites

IV. Conclusions

Modification of Egyptian Bentonite (EB) was carried out using an organo-modifier namely; octadecyl amine (ODA). Polyurethane nanocomposites were synthesized with organically modified EB (Organo Bentonites OB) by in situ polymerization and compositions were prepared by a casting process. OB dispersion of polyurethane nanocomposites was investigated by transmission electron microscopy TEM. A thermogravimetric analyzer (TGA) was used to investigate the decomposition behavior and thermal stability of the cured nanocomposites. The thermal stability of the PNC films was significantly increased with the OB content increment. The complex dielectric permittivity, electrical conductivity, electric modulus, and impedance spectra of the PU/OB nanocomposites were investigated in the frequency range from 0.1 Hz to 10 MHz. The real and imaginary parts of the permittivity decrease with increasing frequency due to an increase in OB content. All the nanocomposites showed relatively low conductivity values and high impedance that could be used for nano-dielectrics.

Acknowledgments:

Authors are grateful to the university of Tabuk for the financial support under research Project Number S-1441-0004.

Declaration of conflicting interests: On behalf of all authors, the corresponding author states that there is no conflict of interest.

References:

[1] Abulyazied DE, Abomostafa HM. J. Inorg. Organomet. Polym. Mater. 2020: 1–12.
[2] Abomostafa HM, Abulyazied DE. J. Inorg. Organomet. Polym. Mater. 2021: 1–13.
[3] Abulyazied DE, Abomostafa HM. J. Compos. Mater. 2021: 00219983211000434.
[4] Maji P, Choudhary RB. Mater. Chem. Phys. 2017; 193: 391–400.
[5] Adak B, Butola BS, Joshi M. Appl. Clay Sci. 2018; 161: 343–353.
[6] Joshi M, Adak B, Butola BS. Prog. Mater. Sci. 2018; 97: 230–282.
[7] Pavlidou S, Papaspyrides CD. Prog. Polym. Sci. 2008; 33(12): 1119–1198.
[8] Masenelli-Varlot K, Chazeau L, Gauthier C, Bogner A, Cavaille J-Y. Compos. Sci. Technol. 2009; 69(10): 1533–1539.
[9] Alexandre M, Dubois P. Mater. Sci. Eng. R Reports 2000; 28(1–2): 1–63.
[10] Page KA, Adachi K. Polymer (Guildf). 2006; 47(18): 6406–6413.
[11] Mogha A. Mater. Today Proc. 2020.
[12] Norouz F, Halabian R, Salimi A, Ghollasi M. Mater. Sci. Eng. C 2019; 103: 109857.
[13] Ramesh S, Punithamoorthy K. J. Mater. Res. Technol. 2019; 8(5): 4173–4181.
[14] Fekry M, Mazrouaa AM, Mohamed MG, Abulyazied DE. Polym. Bull. 2020: 1–27.
[15] Bur AJ, Lee Y-H, Roth SC, Start PR. Polymer (Guildf). 2005; 46(24): 10908–10918.
[16] Yi X, Duan HL, Chen Y, Wang J. Phys. Lett. A 2007; 372(1): 68–71.
[17] Dhatarwal P, Sengwa RJ, Choudhary S. Compos. Commun. 2017; 5: 1–7.
[18] Pissis P, Kripotou S, Kyritsis A. Dielectric Relaxation in Polymer–Clay Nanocomposites. In:. Phys. Prop. Appl. Polym. Nanocomposites. Elsevier 2010; 247–279.
[19] Zilg C, Thomann R, Mülhaupt R, Finter J. Adv. Mater. 1999; 11(1): 49–52.
[20] Yao KJ, Song M, Hourston DJ, Luo DZ. Polymer (Guildf). 2002; 43(3): 1017–1020.
[21] Chen TK, Tien YI, Wei K-H. J. Polym. Sci. Part A Polym. Chem. 1999; 37(13): 2225–2233.
[22] Chen T-K, Tien Y-I, Wei K-H. Polymer (Guildf). 2000; 41(4): 1345–1353.
[23] Motawie AM, Madany MM, El-Dakrory AZ, Osman HM, Ismail EA, Badr MM, El-Komy DA, Abulyazied DE. Egypt. J. Pet. 2014; 23(3): 331–338.
[24] Motawie AM, Madani M, Esmail EA, Dacrorry AZ, Othman HM, Badr MM, Abulyazied DE. Egypt. J. Pet. 2014; 23(4): 379–387.
[25] Subramani S, Choi S-W, Lee J-Y, Kim JH. Polymer (Guildf). 2007; 48(16): 4691–4703.
[26] Gilman JW. Appl. Clay Sci. 1999; 15(1–2): 31–49.
[27] Ramos Filho FG, Mélo TJA, Rabello MS, Silva SML. Polym. Degrad. Stab. 2005; 89(3): 383–392.
[28] Samakande A, Hartmann PC, Cloete V, Sanderson RD. Polymer (Guildf). 2007; 48(6): 1490–1499.
[29] Butkewitsch S, Scheinbeim J. Appl. Surf. Sci. 2006; 252(23): 8277–8286.
[30] Maji P, Choudhary RB, Majhi M. Optik (Stuttg). 2016; 127(11): 4848–4853.
[31] Wong YJ, Hassan J, Hashim M. J. Alloys Compd. 2013; 571: 138–144.
[32] Kaur R, Samra KS. Phys. B Condens. Matter 2018; 538: 29–34.
[33] Chilaka N, Ghosh S. Electrochim. Acta 2014; 134: 232–241.
[34] George S, Varughese KT, Thomas S. J. Appl. Polym. Sci. 1999; 73(2): 255–270.
[35] Zeraati AS, Arjmand M, Sundararaj U. ACS Appl. Mater. Interfaces 2017; 9(16): 14328–14336.
[36] Zhou W, Chen Q, Sui X, Dong L, Wang Z. Compos. Part A Appl. Sci. Manuf. 2015; 71: 184–191.
[37] Zhou W, Zuo J, Ren W. Compos. Part A Appl. Sci. Manuf. 2012; 43(4): 658–664.
[38] Zhou W, Kou Y, Yuan M, Li B, Cai H, Li Z, Chen F, Liu X, Wang G, Chen Q. Compos. Sci. Technol. 2019; 181: 107686.
[39] Madhusudhan CK, Mahendra K, Madhukar BS, Somesh TE, Faisal M. Synth. Met. 2020; 267: 116450.
[40] Choudhary S. Compos. Commun. 2017; 5: 54–63.
[41] Jonscher AK. J. Phys. D. Appl. Phys. 1999; 32(14): R57.